Measurement of the spin-dependent asymmetry in $^3\overrightarrow{\mathrm{He}}(\vec{e},e')$ inelastic scattering at low energy transfer

C. E. Jones
Argonne National Laboratory, Argonne, Illinois 60439

J. Arrington, E. J. Beise,* B. Bray, R. W. Carr, B. W. Filippone, H. Gao,† A. Lung, R. D. McKeown, B. Mueller, and M. L. Pitt
California Institute of Technology, Pasadena, California 91125

D. DeSchepper, G. Dodson, K. Dow, R. Ent,‡ M. Farkhondeh, J.-O. Hansen,§ W. Korsch,‖ L. H. Kramer, K. Lee, N. C. R. Makins,§ R. G. Milner, D. R. Tieger, and T. P. Welch¶
Bates Linear Accelerator Center, Laboratory for Nuclear Science and Department of Physics, Massachusetts Institute of Technology, Cambridge, Massachusetts 02139

E. Candell,** J. Napolitano, C. Tripp, and B. B. Wojtsekhowski‡
Rensselaer Polytechnic Institute, Troy, New York 12180

W. Lorenzon††
TRIUMF, Vancouver, British Columbia, V6T 2A3, Canada
(Received 31 October 1994)

We present the results of a measurement of the spin-dependent asymmetry in $^3\overrightarrow{\mathrm{He}}(\vec{e},e')$ inelastic scattering at kinematics on the low-energy transfer side of the quasielastic peak, including the region near the breakup threshold. Comparison with existing calculations based upon the plane wave impulse approximation shows significant deviation between the data and the model near the breakup threshold. Good agreement between data and theory is seen at higher energy transfer.

PACS number(s): 24.70.+s, 25.10.+s, 25.30.Fj

Because there are as yet no practical free neutron targets, information about the properties of the neutron is often extracted from scattering experiments using nuclear targets, subtracting the contribution from the protons in the nucleus and correcting for reaction mechanisms arising from interactions between the particles within the nucleus. One nucleus used for this purpose is polarized ^{3}He [1]. The basis for the suggestion that polarized ^{3}He makes a good polarized neutron target is the fact that the dominant component of the ground-state wave function is the spatially symmetric, spin-isospin antisymmetric S state in which the spin of the nucleus is carried entirely by the neutron. The D and S' components of the wave function dilute the fraction of the nuclear spin carried by the neutron $(+87\%)$ and contribute a small proton polarization opposite to the nuclear spin direction (-2.7%) [2]. Although the D and S' states constitute a relatively small fraction of the ground-state wave function, these components can contribute a substantial proton signal to the spin-dependent properties.

If one is to extract the neutron properties from experiments using polarized ^{3}He, the nuclear structure of the three-body system and the details of the reaction mechanism must be well understood. Because ^{3}He is a few body nucleus, exact calculations can be performed within a given theoretical model, and theoretical uncertainties associated with extracting the free neutron properties from a nuclear measurement are expected to be small. Until now, quasielastic electron scattering experiments with polarized ^{3}He have concentrated on the kinematic region near the top of the quasielastic peak where the model dependence of extracting the neutron properties from the physical asymmetry is expected to be smallest [3–7]. The existing polarization data are not sufficient both to test the theoretical models and to provide information about the neutron form factors. Additional data from polarized ^{3}He is needed if we are to construct reliable models for extracting the neutron charge form factor G_E^n from experiments using polarized ^{3}He targets.

One kinematic region where measurements of the inclusive inelastic asymmetry are expected to provide significant constraints on theoretical models is the low-energy transfer side of the quasielastic peak. In this region the contribution to the asymmetry from the D state is enhanced relative to the

*Present address: University of Maryland, College Park, MD 20742.
†Present address: University of Illinois, Urbana, IL 61801.
‡Present address: Continuous Electron Beam Accelerator Facility, Newport News, VA 23606.
§Present address: California Institute of Technology, Pasadena, CA 91125.
‖Present address: Argonne National Laboratory, Argonne, IL 60439.
¶Present address: Oregon State University, Corvallis, OR 97331.
**Deceased.
††Present address: University of Pennsylvania, Philadelphia, PA 19104.

top of the quasielastic peak, so measurements are more sensitive to this component of the ^{3}He ground-state wave function which significantly affects the proton contribution to the spin-dependent properties. In addition, final state interactions (FSI) are expected to be large because the final state nucleons have less kinetic energy. Finally, it has been shown that a substantial contribution from meson exchange currents (MEC) is needed to describe the measured elastic electromagnetic form factors of the three-body system [8], so at inelastic kinematics near the elastic peak one can expect to see a contribution from this reaction process. Although no polarization data are available, a measurement of the unpolarized cross section at the two- and three-body breakup thresholds has been made and compared to plane wave impulse approximation (PWIA) calculations and calculations including FSI [9]. The cross section calculations including FSI are in much better agreement with the data. In the immediate threshold region, very large differences (hundreds of percent) between the cross sections obtained from the PWIA and the more sophisticated calculations are seen.

For inclusive quasielastic scattering of longitudinally polarized electrons from a polarized spin$-1/2$ target, the spin-dependent asymmetry is given in terms of the quasielastic response functions as

$$A=-\frac{\cos\theta^* v_{T'}R_{T'}+2\sin\theta^*\cos\phi^* v_{TL'}R_{TL'}}{v_L R_L+v_T R_T}. \quad (1)$$

The v_K are kinematic factors, θ^* and ϕ^* are Euler angles defining the direction of the ^{3}He spin relative to the momentum transfer $\mathbf{q}$, [10] R_L and R_T are the nuclear response functions that describe the unpolarized system, and $R_{T'}$ and $R_{TL'}$ are the spin-dependent response functions. To date, only PWIA calculations of the spin-dependent response functions and the asymmetry in inclusive inelastic scattering have been published [11,12], and this approximation is not necessarily valid, especially outside the region near the top of the quasielastic peak. However, calculations of the unpolarized quasielastic response functions including both FSI and MEC have been reported [13,14]. The work of van Meijgaard and Tjon [14] uses a simplified S wave interaction and cannot be directly extended to describe the spin-dependent properties in $\vec{e}$-$^3\overrightarrow{\mathrm{He}}$ scattering. On the other hand, the model of Schiavilla, Wiringa, and Carlson [13], which includes the spin dependence of the interaction, both FSI and MEC, and treats the wave function and the interaction potential in an internally consistent manner, can be extended to describe spin-dependent scattering in a complete way. Calculations of the spin-dependent response functions within this formalism are underway and initial results for kinematics similar to those reported here show significant effects on $R_{T'}$ and $R_{TL'}$ from both FSI and MEC [15]. Their initial results indicate that the wings of the quasielastic peak are good kinematic regions for tests of the reaction mechanism. In addition, Glöckle *et al.* are calculating the 2- and 3-body breakup processes including FSI and expect sizable corrections in the low energy transfer region [16].

We report here a measurement of the spin-dependent asymmetry at kinematics on the low-energy transfer side of the quasielastic peak. The experiment was performed at the MIT-Bates Linear Accelerator Center using 370 MeV longitudinally polarized electrons. The outgoing electrons were detected in the OHIPS spectrometer at a scattering angle of 70.1°. The ^{3}He target spin quantization direction was 42.5°, which corresponds to $\theta^*=88.1°$ at the top of the quasielastic peak. With this target spin orientation, the experimental asymmetry is sensitive to the interference response function $R_{TL'}$. The kinematic region of the measurement extended from the three-body breakup threshold ($\omega=37.3$ MeV) to $\omega=55.7$ MeV. The spectrometer resolution of 3.5 MeV FWHM does not allow us to distinguish the two- and three-body breakup thresholds in this measurement. The lower limit was chosen sufficiently far from the elastic peak that elastic events did not contribute substantially to the yield. The upper limit was selected to eliminate events near the cutoff in the momentum acceptance of the spectrometer.

The target and polarized source employed for this experiment are described elsewhere [6]. The target, which uses metastability-exchange optical pumping to polarize the ^{3}He nuclei [3], was operated at 12.8 K and 2.15 torr with an effective target length of 10 cm to achieve a target thickness of $1.6\times10^{19}/\mathrm{cm}^2$. The average electron beam current was 25 μA with a polarization of 36.5% as determined by measurements using a Moller polarimeter [17]. The beam helicity was flipped quasirandomly on a pulse-by-pulse basis throughout the experiment and the target spin direction was reversed several times per day to minimize systematic errors. The target polarization was monitored continuously and the beam polarization was measured daily. The systematic uncertainty in the target (beam) polarization is $\Delta P/P=3\%(4\%)$.

The OHIPS spectrometer detector package consists of three planes of plastic scintillators, a crossed wire vertical drift chamber and a gas Čerenkov counter. The raw data trigger required a single hit in all three scintillator planes. Offline cuts for good events included a Čerenkov requirement for pion rejection.

The spectrometer momentum acceptance was $\delta p/p_0=10\%$, which was sufficient to collect events simultaneously from both the elastic peak ($p_{\mathrm{el}}=340.4$ MeV/c) and part of the low-energy transfer side of the quasielastic peak. During the experiment, three different central momentum settings were used; for the purpose of extracting the elastic and inelastic asymmetries from the combined data set, the spectra with the different spectrometer settings were shifted so that the elastic peaks aligned. This was done to a precision of ±0.2 MeV.

The inelastic asymmetry in the analyzed region was split into three bins for the analysis. A number of corrections were applied to extract the physical asymmetry, given in Eq. (1), from the experimental asymmetry. The measured asymmetry was normalized by the target and beam polarizations. Corrections for dilution of the quasielastic cross section from yield from nontarget material and from events in the elastic radiative tail were applied. The asymmetry in the elastic tail was subtracted from the experimental asymmetry. These corrections are described in more detail below and the systematic uncertainty associated with each is shown in Table I. The uncertainties are specified for each energy bin because the inelastic cross section increases rapidly as one goes to higher energy transfer, so that the relative importance of each correction varied substantially with energy. In all instances, the

TABLE I. Systematic uncertainty in the inelastic asymmetry arising from the corrections for the empty target background, the total cross section normalization (σ_{tot}), the yield from the elastic radiative tail (σ_{el}), and the asymmetry in the elastic radiative tail (A_{el}).

ω limits (MeV)	ΔA_{empty} (%)	$\Delta A_{\sigma_{tot}}$ (%)	$\Delta A_{\sigma_{el}}$ (%)	$\Delta A_{A_{el}}$ (%)
37.3−42.1	0.7	0.3	0.1	0.6
42.1−48.7	0.02	0.3	0.2	0.2
48.7−55.7	0.02	0.1	0.09	0.09

total systematic correction was much smaller than the statistical uncertainty in the experimental asymmetry. No inelastic radiative corrections were applied because of lack of reliable calculations of the inelastic asymmetry in this region. Model calculations assuming a reasonable asymmetry distribution that reproduces our experimental results show that these corrections should be much smaller than the statistical uncertainties for all the measured data points.

The only non-negligible sources of background were the target cell walls and windows. Figure 1(a) shows the momentum spectrum with the target full and the target empty.

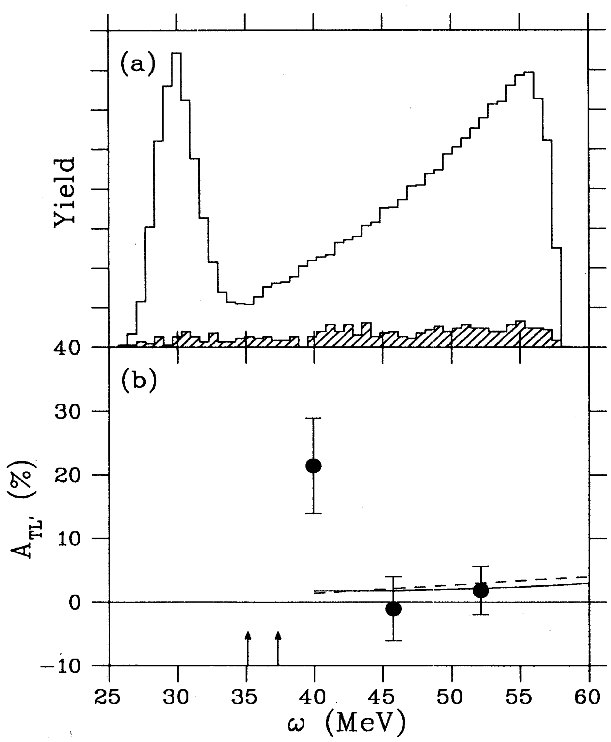

FIG. 1. (a) Relative yield as a function of energy transfer for the target full vs empty. The elastic peak is seen at $\omega = 30$ MeV. (b) Measured inelastic asymmetry as a function of ω on the low energy transfer side of the quasielastic peak. The error bars indicate the statistical uncertainty. The arrows point to the two- and three-body breakup thresholds. The curves correspond to the PWIA calculations of Schulze and Sauer (solid) [21] and Salmé et al. [27] (dashed). No inelastic radiative corrections have been applied to the experimental asymmetries.

TABLE II. Inelastic asymmetry as a function of ω with the systematic and statistical uncertainties shown separately.

ω limits (MeV)	A (%)	ΔA_{stat} (%)	ΔA_{sys} (%)
37.3−42.1	21.4	7.4	1.4
42.1−48.7	−1.1	5.0	0.5
48.7−55.7	1.8	3.8	0.2

The elastic peak, the threshold region, and part of the low ω side of the quasielastic peak are shown. In the region near the inelastic threshold, where the asymmetry is sensitive to background, it is particularly important to have low background yield. In the lowest momentum region used for this data analysis, background from nontarget material contributed less than 15% of the total yield.

It was necessary to determine the total differential cross section in the inelastic region in order to apply corrections for the yield from the elastic tail. Because the three data sets gave slightly different cross sections for this region, for internal consistency the individual data sets were normalized to yield the experimentally known elastic cross section [18] corrected for radiative effects [19]. The normalization factors range from 1.05 to 1.19 for the different data sets. An uncertainty of $\Delta\sigma/\sigma = 15\%$ is assigned to the total cross section in this region to account for uncertainties in the normalization.

Corrections were applied for the asymmetry and yield from the elastic radiative tail. The cross section of the elastic radiative tail was calculated using the procedure of Mo and Tsai [19] separately for each beam helicity, with the asymmetry calculated from the difference in the cross sections for the two beam helicity states. The calculated cross section and asymmetry were momentum averaged to account for the momentum resolution of the spectrometer. An uncertainty of 10% in both cross section and asymmetry is assumed for the calculation of systematic errors. The maximum elastic contribution to the cross section occurs in the lowest energy transfer bin, where 15% of the total rate is attributed to events in the elastic radiative tail. For all energy bins, the correction to the asymmetry for the elastic radiative tail was significantly smaller than the statistical uncertainty.

The measured physics asymmetry as a function of ω is shown in Fig. 1(b). The error bars indicate the statistical uncertainty. Table II shows the experimental asymmetry and the statistical and systematic uncertainties. Because the elastic peak was measured simultaneously, the elastic asymmetry was also extracted. The measured value of $A_{el} = 29.9 \pm 3.9\%$ agrees well with the prediction of 32.1% calculated from fits to experimental data for the elastic form factors [8].

Also shown in Fig. 1(b) are two PWIA calculations for the kinematics of this experiment. The solid line is the calculation of Schulze and Sauer [20] and the dashed line is the calculation of Salmé et al. [21]. As yet no calculations including FSI and MEC are available for comparison with this data. The experimental data agrees well with the PWIA at all but the lowest energy transfer where the experimental asymmetry is larger than the prediction by approximately 3σ. In contrast to PWIA calculations, the experimental data suggests that the asymmetry near the breakup threshold may be large. Such a deviation from the simple reaction mechanism of the PWIA could be a signature for final state interactions or meson exchange currents. Alternatively, it may arise from the ^{3}He ground-state wave function, as it is possible that the two-body breakup part of the reaction is more important than estimated by the calculations in this region. For two-body breakup, the residual nucleus is the deuteron and the nucleon involved in the scattering process is a proton with spin oriented opposite to the spin of the ^{3}He nucleus. A large positive asymmetry is expected for scattering from a polarized proton of this orientation.

In conclusion, we have measured the spin-dependent asymmetry in $^3\overrightarrow{\mathrm{He}}(\vec{e},e')$ inelastic scattering near the breakup threshold. This is the first measurement in this kinematic region and the data complement ongoing theoretical work aimed at understanding the spin properties of few-body systems. The data suggest that near the breakup threshold the inelastic asymmetry may be large, in contradiction with PWIA calculations. This data will serve to constrain more detailed models of the spin-dependent scattering process that include the effects of final state interactions and meson exchange currents.

We would like to thank R.-W. Schulze, G. Salmè, J. Carlson, and R. Schiavilla for providing their calculations, A. Dvoredsky for analyzing the beam polarization data, T. Gentile for valuable discussions about the target, and the staff of the MIT-Bates Linear Accelerator Center. This work was funded by the National Science Foundation Grant Nos. PHY91-15574 (Caltech) and PHY92-08119 (RPI), the U.S. Department of Energy Contract Nos. DE-AC02-76ER03069 (MIT) and W-31-109-ENG-38 (Argonne), and by the Natural Sciences and Engineering Research Council of Canada (TRIUMF).

[1] B. Blankleider and R. M. Woloshyn, Phys. Rev. C **29** (1984), 538.
[2] J. L. Friar, B. F. Gibson, G. L. Payne, A. M. Bernstein, and T. E. Chupp, Phys. Rev. C **42**, 2310 (1990).
[3] C. E. Jones *et al.*, Phys. Rev. C **47**, 110 (1993).
[4] A. K. Thompson *et al.*, Phys. Rev. Lett. **68**, 2901 (1992).
[5] M. Meyerhoff *et al.*, Phys. Lett. B **327**, 201 (1994).
[6] H. Gao *et al.*, Phys. Rev. C **50**, R546 (1994).
[7] J.-O. Hansen *et al.*, Phys. Rev. Lett. **74**, 654 (1995).
[8] A. Amroun, V. Breton, J.-M. Cavedon, B. Frois, D. Goutte, J. Martino, X.-H. Phan, S. K. Platchkov, I. Sick and S. Williamson, Phys. Rev. Lett. **69**, 253 (1992).
[9] G. A. Retzlaff *et al.*, Phys. Rev. C **49**, 1263 (1994).
[10] T. W. Donnelly and A. S. Raskin, Ann. Phys. (N.Y.) **169**, 247 (1986).
[11] R.-W. Schulze and P. U. Sauer, Phys. Rev. C **48**, 38 (1993).
[12] C. Ciofi degli Atti, E. Pace, and G. Salmè, Phys. Rev. C **46**, R1591 (1992); **51**, 1108 (1995).
[13] R. Schiavilla, R. B. Wiringa, and J. Carlson, Phys. Rev. Lett. **70**, 3856 (1993).
[14] E. van Meijgaard and J. A. Tjon, Phys. Rev. C **45**, 1463 (1992); J. A. Tjon, Nucl. Phys. **A546**, 269c (1992).
[15] J. Carlson and R. Schiavilla (private communication).
[16] W. Glöckle (private communication).
[17] J. Arrington, E. J. Beise, B. W. Filippone, T. G. O'Neill, W. R. Dodge, G. W. Dodson, K. A. Dow and J. D. Zumbro, Nucl. Instrum. Methods, Phys. Res. Sect. A **311**, 39 (1992).
[18] J. S. McCarthy, I. Sick, and R. R. Whitney, Phys. Rev. C **15**, 1396 (1977).
[19] L. W. Mo and Y.-S. Tsai, Rev. Mod. Phys. **41**, 205 (1969).
[20] R.-W. Schulze (private communication).
[21] G. Salmé (private communication).